

Reconstructing Neoproterozoic seawater chemistry from early diagenetic dolomite

Peter W. Crockford^{1,2}, Marcus Kunzmann³, Clara L. Blättler⁴, Borianna Calderon-Asael⁵, Jack G. Murphy², Anne-Sofie Ahm², Shlomit Sharoni¹, Galen P. Halverson⁶, Noah J. Planavsky⁵, Itay Halevy¹ and John A. Higgins²

¹Weizmann Institute of Science, Rehovot 76100, Israel

²Department of Geosciences, Princeton University, Princeton, New Jersey 08544, USA

³Commonwealth Scientific and Industrial Research Organisation (CSIRO), Kensington, WA 6151, Australia

⁴Department of Geophysical Sciences, University of Chicago, Chicago, Illinois 60637, USA

⁵Department of Geology and Geophysics, Yale University, New Haven, Connecticut 06511, USA

⁶Department of Earth and Planetary Sciences, McGill University, Montreal, QC H3A 0E8, Canada

ABSTRACT

The pairing of calcium and magnesium isotopes ($\delta^{44/40}\text{Ca}$, $\delta^{26}\text{Mg}$) has recently emerged as a useful tracer to understand the environmental information preserved in shallow-marine carbonates. Here, we applied a Ca and Mg isotopic framework, along with analyses of carbon and lithium isotopes, to late Tonian dolostones, to infer seawater chemistry across this critical interval of Earth history. We investigated the ca. 735 Ma Coppercap Formation in northwestern Canada, a unit that preserves large shifts in carbonate $\delta^{13}\text{C}$ values that have been utilized in global correlations and have canonically been explained through large shifts in organic carbon burial. Under the backdrop of these $\delta^{13}\text{C}$ shifts, we observed positive excursions in $\delta^{44/40}\text{Ca}$ and $\delta^7\text{Li}$ values that are mirrored by a negative excursion in $\delta^{26}\text{Mg}$ values. We argue that this covariation is due to early diagenetic dolomitization of aragonite through interaction with contemporaneous seawater under a continuum of fluid- to sediment-buffered conditions. We then used this framework to show that Tonian seawater was likely characterized by a low $\delta^7\text{Li}$ value of $\sim 13\text{‰}$ ($\sim 18\text{‰}$ lower than modern seawater), as a consequence of a different Li cycle than today. In contrast, $\delta^{13}\text{C}$ values across our identified fluid-buffered interval are similar to modern seawater. These observations suggest that factors other than shifts in global seawater chemistry are likely responsible for such isotopic variation.

INTRODUCTION

Developing a record of seawater chemistry for the majority of Earth's past is dependent on estimating seawater composition from shallow-water (often dolomitized) carbonates. Extracting such global information requires consideration of local processes that decouple shallow-water environments from the global ocean, as well as diagenetic alteration (Banner and Hanson, 1990; Boudreau, 1997; Swart, 2008; Hoffman and Lamothe, 2019). Despite progress in identifying characteristic isotopic markers of early marine diagenesis in carbonates (Ahm et al., 2018; Higgins et al., 2018), ancient strata that show coherent geochemical stratigraphic variability are rarely interpreted within alternative diagenetic frameworks. One interval of Earth history known for high-amplitude $\delta^{13}\text{C}$ variations is the Tonian Period. Based on the apparent preserva-

tion of these variations in multiple successions of the same age, the canonical interpretation is that they record contemporaneous shifts in global marine dissolved inorganic carbon (DIC; Och and Shields-Zhou, 2012). However, this view has recently been challenged by a comprehensive isotopic data set spanning the Otavi carbonate platform and slope succession in Namibia, which shows significant spatial heterogeneity in $\delta^{13}\text{C}$ values across platform to basin transects, suggesting that inner platform records may often better reflect local processes versus global seawater (Hoffman and Lamothe, 2019).

One approach to further understand the geochemical information in dolomites, such as those referenced above, is coupled Ca and Mg isotopes (Fantle and DePaolo, 2007; Fantle and Higgins, 2014; Ahm et al., 2018; Higgins et al., 2018). Early diagenetic Ca isotopic variability in car-

bonates predominantly arises due to sensitivity to water-rock ratios, precipitation rate, and degree of recrystallization or neomorphism. While additional factors, such as temperature and salinity, also impact Ca isotope fractionation between minerals and solution, in general, rapidly precipitated aragonite and calcite (e.g., relevant time scales to the water column) are depleted in ^{44}Ca relative to seawater Ca by $\sim 1.5\text{‰}$ and $\sim 0.9\text{‰}$, respectively (cf. Gussone et al., 2005). However, slow rates of recrystallization and neomorphism, which are characteristic of early marine diagenesis, do not significantly fractionate Ca isotopes (Fantle and DePaolo, 2007). In contrast, dolomite is $\sim 2\text{‰}$ more depleted in ^{26}Mg than dolomitizing solutions (Higgins and Schrag, 2010; Fantle and Higgins, 2014). As a result, depending on Mg availability in pore fluids, Mg can be isotopically distilled during dolomitization. Together, these systems offer the ability to discriminate between Mg-replete fluid-buffered conditions (high $\delta^{44/40}\text{Ca}$, low $\delta^{26}\text{Mg}$, where the chemistry of the carbonate mineral is dictated by the chemistry of the diagenetic fluid) and Mg-poor sediment-buffered conditions (low $\delta^{44/40}\text{Ca}$, high $\delta^{26}\text{Mg}$, where the chemistry of the carbonate mineral is dictated by the chemistry of the sediment) of dolomite formation. Recently, results from Dellinger et al. (2020) suggested that this diagenetic framework can be extended to Li. Here, we applied this approach to reconstruct aspects of Tonian seawater chemistry with implications for the interpretation of shallow-marine carbonate records.

MATERIALS AND METHODS

We analyzed samples from the Coppercap Formation of the Windermere Supergroup (base

of section at 64°37'49.2"N, 129°42'56.8"W) in northwestern Canada (Fig. 1; see the Supplemental Material¹; Aitken, 1981). The study area exposed ~100 m of an ~125 m section, consisting of dolomitic carbonates dominated by matrix-supported debris-flow deposits with centimeter-scale intraclasts (dolofloatstone) and doloturbidite facies with meter-scale fining-upward cycles, deposited in a fault-bounded sub-basin (Fig. 1). In total, we performed 62 $\delta^{44/40}\text{Ca}$ and 66 $\delta^{26}\text{Mg}$ measurements along with trace-element analyses at Princeton University (New Jersey, USA) following the methods of Higgins et al. (2018). We conducted 58 $\delta^7\text{Li}$ measurements at the Yale Geochemistry Center (Yale University, Connecticut, USA) following the methods of Dellinger et al. (2020), and 67 $\delta^{13}\text{C}$ and $\delta^{18}\text{O}$ measurements at McGill University (Montreal, Canada) following the methods of Wörndle et al. (2019) (see the Supplemental Material).

RESULTS

Basal section $\delta^{13}\text{C}$ values begin at -5‰ Vienna Pee Dee belemnite (VPDB) but rise to 0‰

¹Supplemental Material. Extended methods, and explorations into alternative interpretations for these data. Please visit <https://doi.org/10.1130/GEOL.S.13262795> to access the supplemental material, and contact editing@geosociety.org with any questions.

by 45 m, likely correlating with the Russøya negative carbon isotope anomaly (Svalbard; Halverson et al., 2018). Values stay at 0‰ until ~100 m, where they progress toward $+4\text{‰}$. At the same time, $\delta^{44/40}\text{Ca}$ values display $>1\text{‰}$ of variation, with values as low as -1.33‰ (relative to modern seawater) in the lower part of the section (e.g., at 40.5 m) increasing to -0.25‰ (at 72.6 m), and then returning to values near -1‰ at the top of the section (Fig. 1). A similar pattern in $\delta^{44/40}\text{Ca}$ is observed for $\delta^7\text{Li}$ values, but with a range of $\sim 12\text{‰}$, beginning at $\sim +1\text{‰}$ (relative to NIST RM 8545 lithium carbonate standard, L-SVEC) at the base of the section and increasing to almost $+13\text{‰}$ at 80 m and then declining to $+6\text{‰}$ (Fig. 1). Spanning $\sim 1.4\text{‰}$, $\delta^{26}\text{Mg}$ values mirror $\delta^{44/40}\text{Ca}$ and $\delta^7\text{Li}$ trends, beginning at -1.2‰ (relative to Dead Sea Mg, DSM-3) and decreasing to -1.8‰ in the middle of the section and then increasing toward the top of the section (Fig. 1).

DISCUSSION

Stratigraphic covariation among $\delta^{44/40}\text{Ca}$, $\delta^{26}\text{Mg}$, and $\delta^7\text{Li}$ values in the Coppercap Formation (see the Supplemental Material) could either result from synchronous shifts to global Li, Ca, and Mg cycles, or from variability in the style and extent of diagenesis. While it is possible that the residence times of Ca, Mg, and Li were similar across this interval, leading to covarying

shifts in these systems, this is unlikely given their large differences today (Ca $\sim 0.5\text{--}1$ Ma [Fantle and Tipper, 2014]; Mg ~ 10 Ma [Higgins and Schrag, 2015]; Li ~ 1.2 Ma [Misra and Froelich, 2012]). Moreover, mechanisms to explain the amplitude of observed signals and covariation between any two systems fail to explain all three. For $\delta^7\text{Li}$, possible global mechanisms include (1) changes to congruency of continental silicate weathering (Dellinger et al., 2014), (2) varying clay particle–fluid interactions in Li sinks (Li and West, 2014), (3) changes in the flux ratio between high- and low-temperature hydrothermal fluids (Chan et al., 2002), and (4) changes in carbonate polymorphs of primary precipitates (Marriott et al., 2004). However, all of these mechanisms to explain $\delta^7\text{Li}$ trends fail to explain covariation with, and the magnitude of, coeval $\delta^{44/40}\text{Ca}$ and $\delta^{26}\text{Mg}$ values. This is clearly demonstrated through $\delta^{26}\text{Mg}$ values, where, assuming that dolomite formation was secondary, the majority of Mg must have been incorporated after primary precipitates formed and should display variation independent of $\delta^7\text{Li}$ and $\delta^{44/40}\text{Ca}$ trends.

The arguments above motivate alternative explanations for stratigraphic trends in the Coppercap Formation; field observations favor an early marine over late-stage diagenesis interpretation. For example, no heterogeneity in sedimentary facies that may have facilitated

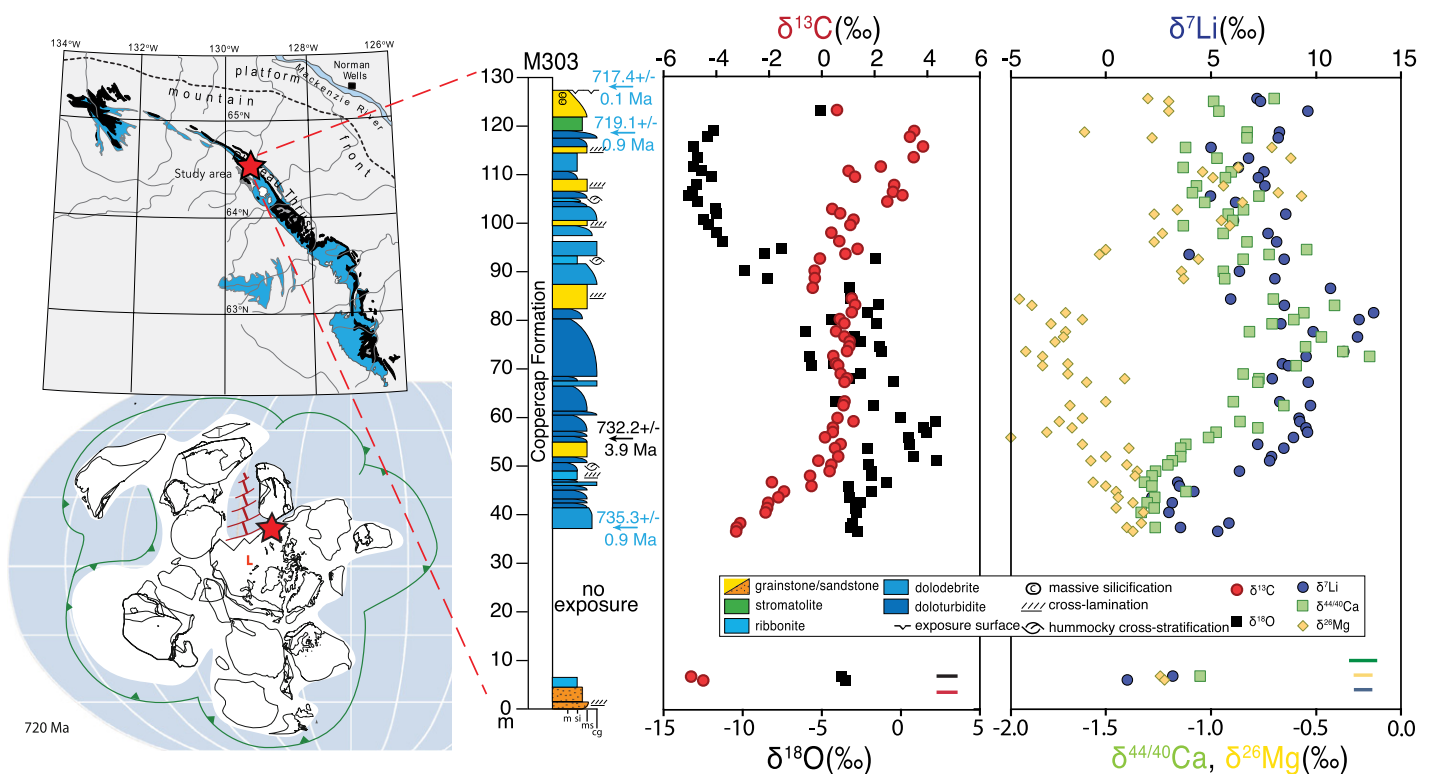


Figure 1. Map of the study area adapted from Crockford et al. (2016), and sedimentary facies stratigraphically plotted with geochemical data. Errors on measurements are in the lower-right corner of panels. Black—Re-Os date measured on a different Coppercap Formation section (Rooney et al., 2014). Blue—U-Pb dates correlated from the Ogilvie Mountains (Yukon, Canada) (upper date; Macdonald et al., 2010) and Ethiopia (MacLennan et al., 2018). Lower left: Reconstruction of Tonian paleogeography; L is Laurentia.

late-stage diagenetic fluid flow is apparent in the study area. Moreover, geochemical variability in the Coppercap Formation occurs over tens of meters and not over the broader spatial scales characteristic of late-stage diagenesis (James and Jones, 2015). In addition, the scale of geochemical stratigraphic variability and the observation of heavy $\delta^{44/40}\text{Ca}$ values are features unlikely to be produced through late-stage diagenesis. Therefore, we interpreted the observed geochemical signals in the context of early marine diagenesis and applied a numerical model following Ahm et al. (2018) to constrain the boundary conditions of the alteration.

Our application of the model was influenced by observations from a modern carbonate platform (Henderson et al., 1999; Higgins et al., 2018; Dellinger et al., 2020) and simulates the dissolution of primary Ca carbonate and reprecipitation as dolomite along a flow path with an evolving fluid composition. Due to the susceptibility of carbonate $\delta^{18}\text{O}$ values to resetting through any fluid interaction, they are less likely to constrain early marine diagenesis and are omitted from further consideration. Model outputs are presented as fields in isotopic cross-plot space between end-member compositions defined by the geochemistry of the primary sediment and the diagenetic dolomite, and between sediment-buffered and fluid-buffered trajectories—of the isotopic systems plotted—that connect end-member compositions (Fig. 2). Model solutions were achieved through estimating the Ca, Li, and Mg concentrations and isotopic compositions of the primary sediment and then finding the diagenetic fluid composition required for the most consistent fit to the measured dolomite data across all phase spaces (Fig. 2; see the Supplemental Material). Departures of data points from the predicted model solution may indicate spatio-temporal heterogeneity in the geochemistry of the primary sediment or of the dolomitizing fluid, which was not resolved by the model. Importantly, because the model does not explicitly account for several carbon-fractionating processes (e.g., aerobic/anaerobic respiration of organic matter or methanogenesis), it

was not expected to capture the entire distribution of observed $\delta^{13}\text{C}$ variability in sediment-buffered carbonates.

Based on our model fit to the data (Fig. 2), we argue that results best reflect diagenetic processes rather than global seawater variation (see the Supplemental Material). From minimum $\delta^{44/40}\text{Ca}$ values and the range of observed $\delta^7\text{Li}$ values, we surmise that the initial carbonate mineral was aragonite, which was then altered by a dolomitizing fluid (Marriott et al., 2004; Blättler and Higgins, 2017). However, we argue that the geochemistry of the dolomitizing fluid was different for the lower portion of the section versus the middle and upper portions. Above ~ 50 m, dolomitization by Tonian seawater (i.e., the same fluid from which the original aragonite formed) places the measured data on model arrays that are well explained by a continuum of fluid- to sediment-buffered conditions displaying similar diagnostic isotopic systematics to modern carbonates that have undergone early marine diagenesis (Higgins et al., 2018; Dellinger et al., 2020). Seawater as the dolomitizing fluid is consistent with the Coppercap Formation's foreslope-like environment, which would have a high potential for open-system fluid-buffered diagenesis by seawater (Hoffman and Lamothe, 2019). The fluid-buffered samples (~ 50 – 90 m) suggest that Tonian seawater had a $\delta^7\text{Li}$ value of $\sim 13\text{‰}$, a near-modern $\delta^{44/40}\text{Ca}$ value (0‰), and enough Mg such that dolomitization did not appreciably distill Mg isotopes (Fig. 2). The isotopic composition of the sediment-buffered interval (~ 90 – 125 m) is consistent with aragonite that precipitated from the proposed Tonian seawater, followed by dolomitization during early marine diagenesis under relatively closed-system conditions that allowed for Mg drawdown and Mg-isotopic distillation in the diagenetic fluid.

Data from the lower half of the section (~ 0 – 50 m) fall off the arrays that explain the variation in the upper half of the section, displaying lower $\delta^{44/40}\text{Ca}$ and $\delta^7\text{Li}$ values (Fig. 2). The isotopic composition of these samples is well explained by sediment-buffered diagenesis of aragonite that

formed out of Tonian seawater by a dolomitizing fluid that was a mixture of brackish groundwater and Tonian seawater (Fig. S7). We suggest that groundwater flow through the carbonate sediments on the shelf and slope resulted in a relatively Mg- and Li-poor, CaCO_3 -saturated solution, which, when mixed with the proposed Tonian seawater, produced a dolomitizing fluid that well explains the lower half of the section (Supplemental Material). It seems less plausible that the dolomitizing fluid of the lower half of the section was purely seawater of a different chemical and isotopic composition, given the required changes in the concentrations and/or isotopic compositions, and the time available to realize these changes (Supplemental Material).

Although we contend that chemostratigraphic variability in the Coppercap Formation reflects variable diagenetic conditions and not variations in seawater chemistry, this analysis still yields important insights into late Tonian Li and carbon cycles. Across the fluid-buffered interval, $\delta^7\text{Li}$ values approach $\sim 13\text{‰}$, which we argue is likely a close approximation of the $\delta^7\text{Li}$ composition of late Tonian seawater (Dellinger et al., 2020). A $\delta^7\text{Li}$ of $\sim 13\text{‰}$ is significantly different from modern seawater (31‰ ; Tomaschak, 2004), possibly as a consequence of lower riverine $\delta^7\text{Li}$ values due to more congruent continental silicate weathering before the rise of land plants (Kalderon et al., 2016) and potentially analogous to extreme weathering intervals of the Phanerozoic such as the Permian-Triassic extinction (Sun et al., 2018). Additionally, the Precambrian ocean would have been silica-rich (Drever, 1974) due to the absence of silicifying marine organisms, favoring authigenic clay formation (Isson et al., 2020). Because authigenic clay formation in marine sediments and off-axis alteration are the major Li sinks (Misra and Froelich, 2012), increased clay formation would likely result in a lower seawater Li concentration. Lower seawater Li concentrations would favor near-quantitative Li uptake in marine sediments and off-axis hydrothermal systems, muting the effect of preferential ^6Li uptake in these environments (Chan et al., 2002), with the net ef-

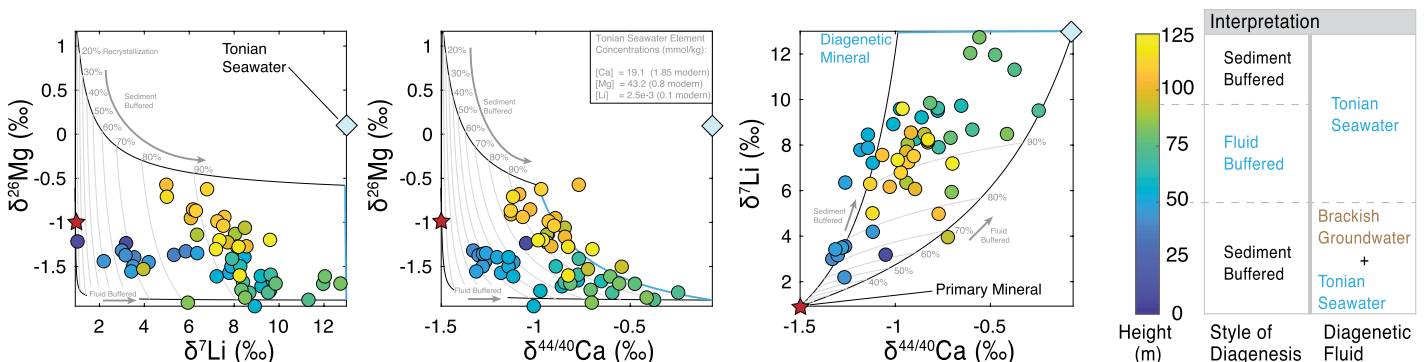


Figure 2. $\delta^{26}\text{Mg}$, $\delta^7\text{Li}$, and $\delta^{44/40}\text{Ca}$ cross-plots with model solutions. Grid lines represent percent alteration in 10% increments. Red stars represent primary aragonite, and blue lines represent final diagenetic product. Blue diamonds are proposed Tonian seawater.

fect of lowering Tonian $\delta^7\text{Li}$ values compared to Cenozoic seawater (Misra and Froelich, 2012).

The fluid-buffered interval of the Coppercap Formation can constrain the Tonian marine DIC reservoir as well. Carbonate $\delta^{13}\text{C}$ values across these intervals are indistinguishable from modern DIC at $\sim 0\text{‰}$ (Fig. 1). In contrast, large variability (-5‰ to $+4\text{‰}$) is observed across sediment-buffered intervals. Given the isotopic evidence for diagenetic alteration of major constituents of the carbonate rock (Ca, Mg), it seems reasonable that carbon would have been subjected to a similar diagenetic fate. Variation of $\delta^{13}\text{C}$ values in the sediment-buffered intervals may have resulted from organic matter remineralization or methanogenesis in the sediments or from variable degrees of local carbon-isotope distillation of DIC across the platform (Swart, 2008; Geyman and Maloof, 2019). In contrast, the fluid-buffered intervals may offer a more robust picture of Tonian seawater carbonate chemistry.

Evaluation of local versus global controls on chemostratigraphic records in shallow-marine carbonates may be achieved by wider application of the paired Ca-Mg isotope framework. This evaluation may be best executed by targeting environments with the greatest potential to record seawater-buffered early marine diagenesis (i.e., the flanks of carbonate platforms and slopes; Hoffman and Lamothe, 2019). If identified fluid-buffered intervals display geochemical variability (e.g., $\delta^{13}\text{C}$, $\delta^7\text{Li}$, $\delta^{44/40}\text{Ca}$, $\delta^{26}\text{Mg}$) similar to sediment-buffered intervals, then this will provide confidence in shallow-marine carbonate archives as records of seawater geochemical evolution. However, if a significant offset between fluid- and sediment-buffered intervals is the norm, a more thorough screening of the existing shallow-marine carbonate record to identify fluid-buffered intervals will be necessary to reconstruct the secular evolution of seawater chemistry. In the case of the Coppercap Formation, results suggest that Tonian marine DIC $\delta^{13}\text{C}$ may not have varied to the degree that is suggested by shallow-marine carbonate archives, adding to a growing call for a reinterpretation of such records.

ACKNOWLEDGMENTS

Crockford acknowledges support from the Natural Sciences and Engineering Research Council of Canada (NSERC) CREATE CATP program, the Agouron Institute (Pasadena, California, USA), and McGill University (Montreal, Canada). Halverson acknowledges support from NSERC. Halevy acknowledges support from European Research Council grant 755053. Higgins and Blättler were supported by Simons Foundation (New York, USA) Award 339006, and Planavsky acknowledges support from the Alternative Earths National Aeronautics and Space Administration (NASA) Astrobiology Institute. We thank Paul F. Hoffman and three anonymous reviewers for insightful comments, which greatly improved this manuscript.

REFERENCES CITED

Ahm, A.S.C., Bjerrum, C.J., Blättler, C.L., Swart, P.K., and Higgins, J.A., 2018, Quantifying ear-

ly marine diagenesis in shallow-water carbonate sediments: *Geochimica et Cosmochimica Acta*, v. 236, p. 140–159, <https://doi.org/10.1016/j.gca.2018.02.042>.

Aitken, J.D., 1981, Stratigraphy and sedimentology of the Upper Proterozoic Little Dal Group, Mackenzie Mountains, Northwest Territories, in Campbell, F.H.A., ed., *Proterozoic Basins of Canada*: Geological Survey of Canada Paper 81, p. 47–71.

Banner, J.L., and Hanson, G.N., 1990, Calculation of simultaneous isotopic and trace element variations during water-rock interaction with applications to carbonate diagenesis: *Geochimica et Cosmochimica Acta*, v. 54, p. 3123–3137, [https://doi.org/10.1016/0016-7037\(90\)90128-8](https://doi.org/10.1016/0016-7037(90)90128-8).

Blättler, C.L., and Higgins, J.A., 2017, Testing Urey's carbonate-silicate cycle using the calcium isotopic composition of sedimentary carbonates: *Earth and Planetary Science Letters*, v. 479, p. 241–251, <https://doi.org/10.1016/j.epsl.2017.09.033>.

Boudreau, B.P., 1997, *Diagenetic Models and Their Implementation*: Berlin, Springer, 414 p., <https://doi.org/10.1007/978-3-642-60421-8>.

Chan, L.H., Alt, J.C., and Teagle, D.A., 2002, Lithium and lithium isotope profiles through the upper oceanic crust: A study of seawater-basalt exchange at ODP Sites 504B and 896A: *Earth and Planetary Science Letters*, v. 201, p. 187–201, [https://doi.org/10.1016/S0012-821X\(02\)00707-0](https://doi.org/10.1016/S0012-821X(02)00707-0).

Crockford, P.W., et al., 2016, Triple oxygen and multiple sulfur isotope constraints on the evolution of the post-Marinoan sulfur cycle: *Earth and Planetary Science Letters*, v. 435, p. 74–83, <https://doi.org/10.1016/j.epsl.2015.12.017>.

Dellinger, M., Gaillardet, J., Bouchez, J., Calmels, D., Galy, V., Hilton, R.G., Louvat, P., and France-Lanord, C., 2014, Lithium isotopes in large rivers reveal the cannibalistic nature of modern continental weathering and erosion: *Earth and Planetary Science Letters*, v. 401, p. 359–372, <https://doi.org/10.1016/j.epsl.2014.05.061>.

Dellinger, M., Hardisty, D.S., Planavsky, N.H., Gill, B.C., Kalderon-Asael, B., Asael, D., Croissant, T., Swart, P.K., and West, A.J., 2020, The effects of diagenesis on lithium isotope ratios of shallow marine carbonates: *American Journal of Science*, v. 320, p. 150–184, <https://doi.org/10.2475/02.2020.03>.

Drever, J.I., 1974, Geochemical model for the origin of Precambrian banded iron formations: *Geological Society of America Bulletin*, v. 85, p. 1099–1106, [https://doi.org/10.1130/0016-7606\(1974\)85<1099:GMFTOO>2.0.CO;2](https://doi.org/10.1130/0016-7606(1974)85<1099:GMFTOO>2.0.CO;2).

Fantle, M.S., and DePaolo, D.J., 2007, Ca isotopes in carbonate sediment and pore fluid from ODP Site 807A: The $\text{Ca}^{2+}_{(\text{aq})}$ -calcite equilibrium fractionation factor and calcite recrystallization rates in Pleistocene sediments: *Geochimica et Cosmochimica Acta*, v. 71, p. 2524–2546, <https://doi.org/10.1016/j.gca.2007.03.006>.

Fantle, M.S., and Higgins, J., 2014, The effects of diagenesis and dolomitization on Ca and Mg isotopes in marine platform carbonates: Implications for the geochemical cycles of Ca and Mg: *Geochimica et Cosmochimica Acta*, v. 142, p. 458–481, <https://doi.org/10.1016/j.gca.2014.07.025>.

Fantle, M.S., and Tipper, E.T., 2014, Calcium isotopes in the global biogeochemical Ca cycle: Implications for development of a Ca isotope proxy: *Earth-Science Reviews*, v. 129, p. 148–177, <https://doi.org/10.1016/j.earscirev.2013.10.004>.

Geyman, E.C., and Maloof, A.C., 2019, A diurnal carbon engine explains ^{13}C -enriched carbonates without increasing the global production of oxygen: *Proceedings of the National Academy of Sciences of the United States of America*, v. 116, p. 24433–24439, <https://doi.org/10.1073/pnas.1908783116>.

Gussone, N., Böhm, F., Eisenhauer, A., Dietzel, M., Heuser, A., Teichert, B.M., Reitner, J., Wörheide, G., and Dullo, W.C., 2005, Calcium isotope fractionation in calcite and aragonite: *Geochimica et Cosmochimica Acta*, v. 69, p. 4485–4494, <https://doi.org/10.1016/j.gca.2005.06.003>.

Halverson, G.P., Porter, S.M., and Gibson, T.M., 2018, Dating the late Proterozoic stratigraphic record: *Emerging Topics in Life Sciences*, v. 2, p. 137–147, <https://doi.org/10.1042/ETLS20170167>.

Henderson, G.M., Slowey, N.C., and Haddad, G.A., 1999, Fluid flow through carbonate platforms: Constraints from $^{234}\text{U}/^{238}\text{U}$ and Cl⁻ in Bahamas pore-waters: *Earth and Planetary Science Letters*, v. 169, p. 99–111, [https://doi.org/10.1016/S0012-821X\(99\)00065-5](https://doi.org/10.1016/S0012-821X(99)00065-5).

Higgins, J.A., and Schrag, D.P., 2010, Constraining magnesium cycling in marine sediments using magnesium isotopes: *Geochimica et Cosmochimica Acta*, v. 74, p. 5039–5053, <https://doi.org/10.1016/j.gca.2010.05.019>.

Higgins, J.A., and Schrag, D.P., 2015, The Mg isotopic composition of Cenozoic seawater—Evidence for a link between Mg-clays, seawater Mg/Ca, and climate: *Earth and Planetary Science Letters*, v. 416, p. 73–81, <https://doi.org/10.1016/j.epsl.2015.01.003>.

Higgins, J.A., et al., 2018, Mineralogy, early marine diagenesis, and the chemistry of shallow-water carbonate sediments: *Geochimica et Cosmochimica Acta*, v. 220, p. 512–534, <https://doi.org/10.1016/j.gca.2017.09.046>.

Hoffman, P.F., and Lamothe, K.G., 2019, Seawater-buffered diagenesis, destruction of carbon isotope excursions, and the composition of DIC in Neoproterozoic oceans: *Proceedings of the National Academy of Sciences of the United States of America*, v. 116, p. 18874–18879, <https://doi.org/10.1073/pnas.1909570116>.

Isson, T.T., Planavsky, N.J., Coogan, L.A., Stewart, E.M., Ague, J.J., Bolton, E.W., Zhang, S., McKenzie, N.R., and Kump, L.R., 2020, Evolution of the global carbon cycle and climate regulation on Earth: *Global Biogeochemical Cycles*, v. 34, p. e2018GB006061, <https://doi.org/10.1029/2018GB006061>.

James, N.P., and Jones, B., 2015, *Origin of Carbonate Sedimentary Rocks*: New York, John Wiley & Sons, 464 p.

Kalderon, B., Planavsky, N., and Asael, D., 2016, A carbonate Li isotope record throughout Earth history: *Goldschmidt Conference, Yokohama, Japan, 26 June to 1 July, Abstract 1410*.

Li, G., and West, A.J., 2014, Evolution of Cenozoic seawater lithium isotopes: Coupling of global denudation regime and shifting seawater sinks: *Earth and Planetary Science Letters*, v. 401, p. 284–293, <https://doi.org/10.1016/j.epsl.2014.06.011>.

Macdonald, F.A., Schmitz, M.D., Crowley, J.L., Roots, C.F., Jones, D.S., Maloof, A.C., Strauss, J.V., Cohen, P.A., Johnston, D.T., and Schrag, D.P., 2010, Calibrating the Cryogenian: *Science*, v. 327, p. 1241–1243, <https://doi.org/10.1126/science.1183325>.

MacLennan, S., Park, Y., Swanson-Hysell, N., Maloof, A., Schoene, B., Gebreslassie, M., Antilla, E., Tesema, T., Alene, M., and Haileab, B., 2018, The arc of the snowball: U-Pb dates constrain the Islay anomaly and the initiation of the Sturtian glaciation: *Geology*, v. 46, p. 539–542, <https://doi.org/10.1130/G40171.1>.

Marriott, C.S., Henderson, G.M., Crompton, R., Staubwasser, M., and Shaw, S., 2004, Effect of mineralogy, salinity, and temperature on Li/Ca and Li isotope composition of calcium carbonate: *Chemical Geology*, v. 212, p. 5–15, <https://doi.org/10.1016/j.chemgeo.2004.08.002>.

- Misra, S., and Froelich, P.N., 2012, Lithium isotope history of Cenozoic seawater: Changes in silicate weathering and reverse weathering: *Science*, v. 335, p. 818–823, <https://doi.org/10.1126/science.1214697>.
- Och, L.M., and Shields-Zhou, G.A., 2012, The Neoproterozoic oxygenation event: Environmental perturbations and biogeochemical cycling: *Earth-Science Reviews*, v. 110, p. 26–57, <https://doi.org/10.1016/j.earscirev.2011.09.004>.
- Rooney, A.D., Macdonald, F.A., Strauss, J.V., Dudás, F.Ö., Hallmann, C., and Selby, D., 2014, Re-Os geochronology and coupled Os-Sr isotope constraints on the Sturtian snowball Earth: *Proceedings of the National Academy of Sciences of the United States of America*, v. 111, p. 51–56, <https://doi.org/10.1073/pnas.1317266110>.
- Sun, H., Xiao, Y., Gao, Y., Zhang, G., Casey, J.F., and Shen, Y., 2018, Rapid enhancement of chemical weathering recorded by extremely light seawater lithium isotopes at the Permian-Triassic boundary: *Proceedings of the National Academy of Sciences of the United States of America*, v. 115, p. 3782–3787, <https://doi.org/10.1073/pnas.1711862115>.
- Swart, P.K., 2008, Global synchronous changes in the carbon isotopic composition of carbonate sediments unrelated to changes in the global carbon cycle: *Proceedings of the National Academy of Sciences of the United States of America*, v. 105, p. 13741–13745, <https://doi.org/10.1073/pnas.0802841105>.
- Tomascak, P.B., 2004, Developments in the understanding and application of lithium isotopes in the earth and planetary sciences: *Reviews in Mineralogy and Geochemistry*, v. 55, p. 153–195, <https://doi.org/10.2138/gsrmg.55.1.153>.
- Wörndle, S., Crockford, P.W., Kunzmann, M., Bui, T.H., and Halverson, G.P., 2019, Linking the Bitter Springs carbon isotope anomaly and early Neoproterozoic oxygenation through I/[Ca+ Mg] ratios: *Chemical Geology*, v. 524, p. 119–135, <https://doi.org/10.1016/j.chemgeo.2019.06.015>.

Printed in USA